Catalysis Communications 92 (2017) 15–18

Contents lists available at ScienceDirect

Catalysis Communications

journal homepage: www.elsevier.com/locate/catcom

Short communication

Enhanced removal of toluene by dielectric barrier discharge coupling with Cu-Ce-Zr supported ZSM-5/TiO_2/Al_2O_3

Baojuan Dou [a], Deliang Liu [a], Qing Zhang [a], Ruozhu Zhao [a], Qinglan Hao [a], Feng Bin [b,*], Jingguo Cao [a,*]

[a] Tianjin University of Science & Technology, Tianjin 300457, China
[b] State Key Laboratory of High-Temperature Gas Dynamics, Institute of Mechanics, Chinese Academy of Sciences, Beijing 100190, China

ARTICLE INFO

Article history:
Received 10 October 2016
Received in revised form 16 December 2016
Accepted 19 December 2016
Available online 21 December 2016

Keywords:
Dielectric barrier discharge
Cu-Ce-Zr catalyst
Catalyst characterization
Toluene

ABSTRACT

Toluene was removed by dielectric barrier discharge coupling with Cu-Ce-Zr supported ZSM-5/TiO_2/Al_2O_3 catalysts. Copper, cerium, and zirconium species were highly dispersed on the support surface, and copper was mostly in Cu^{2+} and Cu^{+} state co-existed. The reaction process of toluene removal in the plasma-catalyst system was influenced by the support of the catalyst and it could be divided into three steps. Pure plasma and thermal catalytic chemistry triggered by background temperature played different roles in the different step. Large pore size, more oxygen vacancy and lattice oxygen in the CuCeZr/TiO_2 were responsible to the excellent toluene removal, CO_2 selectivity and energy yield.

1. Introduction

Because volatile organic compounds (VOCs) are hazardous to human health, contributing to serious environmental problems such as the organic aerosols, photochemical oxidants and ground level ozone [1,2], extensive research was focused on the development of control technologies to limit VOCs emissions. Non-thermal plasma (NTP) has received considerable attentions due to the great advantages of achievement of high electron energies within short residence time and easy operations under ambient temperature. However, pure NTP suffers from weaknesses of incomplete oxidation with emission of harmful by-products, poor energy efficiency and low mineralization degree [3]. More effective use of NTP is by exploiting its potential via the combination with heterogeneous catalysis, with advantages for the quick response from plasma and high selectivity of desired products from catalysis. Moreover, incomplete oxidation with emission of harmful compounds can be inhibited by the development of a suitable catalyst [4].

Cu-based catalysts are widely used in the VOCs oxidation for their high efficiencies, especially when doped with other metals, such as Ce and Zr. CeO_2 has been regarded as an effective promoter in thermal catalytic reactions because of its high oxygen storage capacities and redox properties between Ce^{4+} and Ce^{3+} [5]. Zhu et al. [6] found that the interaction between Cu and Ce species resulting in greater formation of surface adsorbed oxygen that favors the oxidation of formaldehyde in the plasma process. Bin et al. [7] and Rivas et al. [8] confirmed that the dispersion and stability of active metals can be improved by adding of zirconia to metal-based catalysts through strong metal-support interactions.

Whereas, unsupported metal oxides catalysts may exhibit disadvantages of weak mechanical, strength poor thermal stability and low surface areas, which consequently limit their practical applications. Fortunately, the function of a catalyst support can offset those defects. More importantly, the structure and the interaction between the support and the active metals can influence catalytic activity. In our previous study, the supported catalyst of CuCeZr/ZSM-5 with Ce/Zr molar ratio of 3 was proved to have the best activity for thermal catalytic oxidation of VOCs [9]. However, very limited attention has been focused on the study of Ce-Zr promoted copper based catalyst in the NTP-catalyst combined system for the removal of VOCs so far. And, it is of great significance to investigate the influence of support on the Ce-Zr promoted copper based catalysts in the field of VOCs removal by using plasma coupled with catalyst.

In this work, a series of Cu-Ce-Zr based catalysts supported on ZSM-5, γ-Al_2O_3 and TiO_2 were prepared by using an incipient wetness impregnation method. A dielectric barrier discharge (DBD) reactor was used to generate plasma and the catalysts were placed into the discharge zone. Toluene as a typical aromatics vast existed in industrial processes, was adopted as the probe pollutant. The enhanced degradation behaviors of toluene by DBD coupling with the catalysts were investigated in terms of toluene removal and CO_2 selectivity. Combined with characterization techniques, the synergistic effect of plasma and the catalyst at each stage of toluene removal over different catalysts in plasma-catalyst system will be analyzed deeply.

* Corresponding authors.
E-mail addresses: binfeng@imech.ac.cn (F. Bin), cjg@tust.edu.cn (J. Cao).

http://dx.doi.org/10.1016/j.catcom.2016.12.024
1566-7367/

2. Experimental

2.1. Catalyst preparation

The CuCeZr/ZSM-5 (CuCeZr/Z), CuCeZr/TiO_2 (CuCeZr/T) and CuCeZr/γ-Al_2O_3 (CuCeZr/A) catalysts were prepared by incipient wetness impregnation method. The copper content of all the catalysts was fixed at 4 wt%, and the molar ratio of Cu: Ce: Zr was 1: 0.75: 0.25. The experimental details of catalysts preparation were described in detail in Supplementary data.

2.2. Catalyst characterization

Experimental details for N_2 adsorption-desorption, powder X-ray diffraction (XRD), X-ray photoelectron spectroscopy (XPS) and hydrogen temperature programmed reduction (H_2-TPR) were described in detail in Supplementary data.

2.3. Experimental set-up

The experimental set-up of VOCs degradation by plasma-catalysis was described in Fig.S1, including continuous flow gas supplying system, DBD reactor and gaseous analytical systems. The flow rate and toluene concentration were fixed at 1 L/min and 1400 ppm, respectively, with the space velocity of 10,000 h^{-1}. The experimental details for experimental set-up were described in Supplementary data. The removal of toluene was obtained by the following equation:

$$\mathrm{Con.}(\%) = \frac{C_{in} - C_{out}}{C_{in}} \times 100\% \quad (1)$$

where C_{in} is the inlet molar flow rate of VOCs, C_{out} is the outlet molar flow rate of VOCs. The selectivity of CO_2 is defined as follows:

$$S_{CO_2}(\%) = \frac{C_{CO_2}}{7 \times (C_{in} - C_{out})} \quad (2)$$

where C_{in} and C_{out} are the inlet and outlet concentrations of toluene, respectively. C_{CO_2} is the out concentrations of CO_2.

3. Results and discussion

3.1. Characterizations

Textural properties of all the fresh Cu-Ce-Zr based catalysts are shown in Fig. S2 and Table S1. Compared with CuCeZr/Z and CuCeZr/A, CuCeZr/T possesses largest pore size (10–180 nm) and the lowest surface area (25 m^2/g). The specific surface area (295 m^2/g) of CuCeZr/Z is the highest, while the pore size (0.37 nm) is too small for the diffusion of VOCs molecules. The XRD powder patterns of the Cu-Ce-Zr based catalysts with different supports are depicted in Fig. S3. The characteristic peaks at 2θ = 7.9, 8.9, 23.1 and 24.1° for ZSM-5, 2θ = 46.5, 67.3° for γ-Al_2O_3, and 2θ = 25.3, 37.8, 48, 54.9, 62.8° for TiO_2 can be found for CuCeZr/Z, CuCeZr/A and CuCeZr/T catalysts, respectively. The results indicate that the supports still maintain their structural characteristics after the copper, cerium and zirconium being loaded. For all the catalysts, no diffraction peaks corresponding to CuO and ZrO_2 are observed, suggesting that copper and zirconium species are homogeneously dispersed on the supports. While faint diffraction peak at 2θ = 29° attributed to CeO_2 can be found for all catalysts, indicative of the low crystallinity of CeO_2 [10].

XPS analysis was performed in order to obtain the chemical states and surface compositions of elements in the Cu-Ce-Zr based catalysts, as shown in Fig. 1 and Table S2. Cu 2p XPS spectra (Fig. 1A) show two main peaks of Cu $2p_{3/2}$ and Cu $2p_{1/2}$ at about 934.0 and 954.8 eV, respectively. The shake-up peaks located in the range of 937.5–947.5 eV demonstrate the existence of divalent copper. After the peak deconvolution and fitting, the higher Cu $2p_{3/2}$ binding energy and the presence of shake-up peak are the two important XPS characteristics of Cu^{2+} existence, while the lower Cu $2p_{3/2}$ binding energy is the characteristic of the reduced copper species (main Cu^+). The Cu^{2+}/Cu^+ ratio for CuCeZr/T is the lowest indicating the most reduced Cu species existing in CuCeZr/T (Table S2).

The Ce 3d spectra of catalysts (Fig. 1B) are individually deconvoluted into $3d_{5/2}$ and $3d_{3/2}$ spin-orbit components (labeled as *v* and *u*, respectively), which describes the $Ce^{4+} \leftrightarrow Ce^{3+}$ electronic transitions. The main peaks at about 882.8 (v), 889.1 (v_2), and 898.5 eV (v_3) can be attributed to Ce^{4+} $3d_{5/2}$, and the peaks at about 901 (u), 908.5 (u_2) and 916.8 (u) eV are resulted from Ce^{4+} $3d_{3/2}$, indicating the Ce 3d core level is dominated by the contributions from Ce^{4+} cations [11]. The other two peaks at 884.5 eV (v_1) and 904.1 eV (u_1) can be assigned to Ce^{3+} $3d_{5/2}$ and Ce^{3+} $3d_{3/2}$, respectively. From Table S2, it is evident that cerium is mostly in a Ce^{4+} oxidation state, with a small quantity of Ce^{3+} co-existed. It is reported that the existence of Ce^{3+} in CeO_2 implies the formation of an oxygen vacancy, and subsequently increasing catalytic activity [12]. Moreover, the generation of Cu^+ together with Ce^{3+} is indicative of the redox equilibrium ($Ce^{3+} + Cu^{2+} \leftrightarrow Ce^{4+} + Cu^+$), which is claimed to be the enhancement of reduced copper species [13].

The Zr 3d XPS spectra of all the catalysts shows two main peaks in Fig. 1C: a peak at approximately 182.1 eV that can be attributed to Zr $3d_{5/2}$, and a peak at about 184.5 eV that can be ascribed to Zr $3d_{3/2}$, which corresponds to the Zr^{4+}. For all the samples, no obvious difference for the zirconium binding energy can be observed.

The O 1s XPS spectra of the catalysts are shown in Fig. 1D. After deconvolution and fitting, the existence of two peaks indicates the presence of two different kinds of oxygen species. The peak at approximately 530 eV can be assigned to lattice oxygen (O_{latt}) associated with copper, cerium and zirconium metal oxides, while the peak at a higher binding energy (531.5 eV) can be attributed to surface adsorbed oxygen (O_{ad}) and weekly bonded oxygen species [14]. Combined with the results from Table S2, the O_{latt} / (O_{ad} + O_{latt}) ratio of CuCeZr/T is the highest, which is an evidence for providing of lattice oxygen by the TiO_2 support [15].

Fig. 2 presents the H_2-TPR profiles of CuCeZr/T, CuCeZr/Z and CuCeZr/A. Three main reduction peaks, denoted as α, β and γ, were identified in the CuCeZr/Z and CuCeZr/T, while two reductive peaks (α and β) were detected in CuCeZr/A. The α peak is generally proposed as the reduction of well dispersed copper species on the support, and the β peak can be attributed to the reduction of the copper oxide adhering to the external surface of the support, while the γ peak is associated with the reduction of the bulk copper oxide [16,17]. The temperature of α peaks for CuCeZr/T (152 °C) and CuCeZr/Z (158 °C) are lower than CuCeZr/Z (173 °C), while the corresponding H_2 consumption for CuCeZr/T (1500 μmol·g^{-1}) is the highest (Table S2).

3.2. Toluene removal by DBD coupling with catalyst

Toluene removal using DBD coupling with CuCeZr/Z, CuCeZr/A and CuCeZr/T was investigated (Fig. 3). Obviously, toluene removal and CO_2 selectivity in the plasma-catalyst system are significantly higher than those in pure NTP system. In particular, with the discharge power higher than 26 W, CO_2 selectivity increases slowly and stabilized at about 40%, while the removal rate of toluene increases rapidly from 35.4% to 78.8%. Improving discharge power can enhance the intensity of electric field generating more electrons, radicals, neutral particles and ions, which can non-selectively decompose toluene molecules. Therefore, pure NTP can obtain high removal rate of VOCs but low mineralization degree.

For the plasma-catalyst system, toluene removal and CO_2 selectivity increase with discharge power, and it was influenced by the support of the catalyst. It is evidenced that toluene removal and CO_2 selectivity for

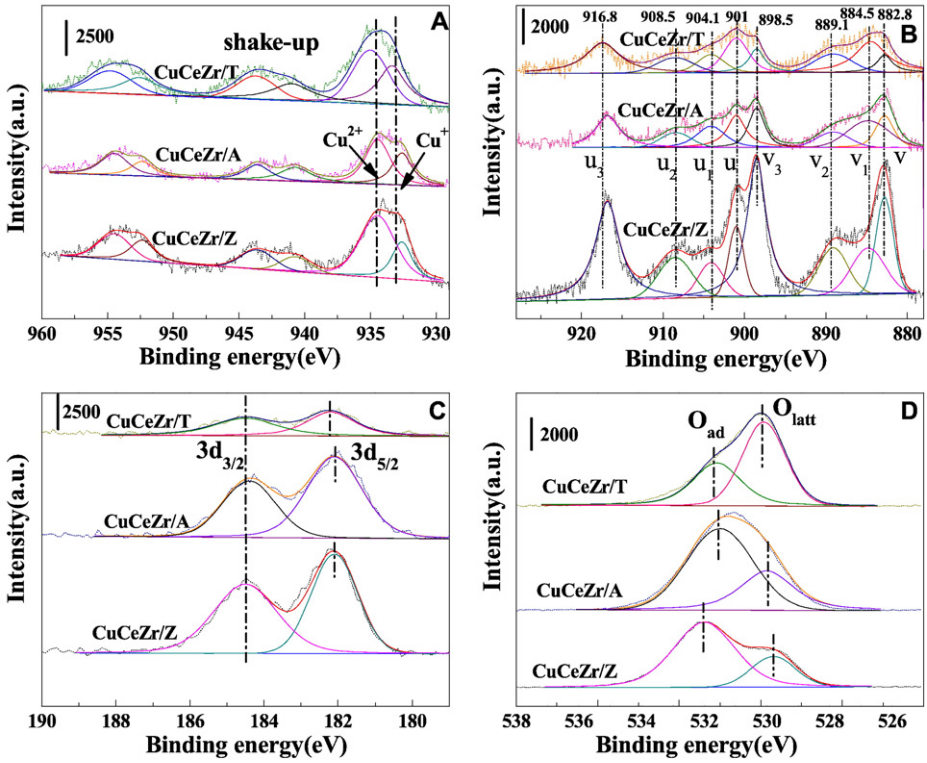

Fig. 1. XPS narrow spectra of Cu 2p (A), Ce 3d (B), Zr 3d (C) and O 1 s (D) for catalysts.

CuCeZr/Z are lower compared with CuCeZr/A and CuCeZr/T, probably owing to the micropore size of CuCeZr/Z (0.37 nm) much smaller than toluene molecule (0.67 nm), and weak reducibility in low temperature and less lattice oxygen. In addition, micropores in CuCeZr/Z limit the developing of micro-discharge inside the pores and only surface discharge formed [18,19], and thus weaker electric field caused low toluene removal.

For CuCeZr/A and CuCeZr/T, the reaction process of toluene removal in plasma-catalyst system, can be divided into three steps in this study. The first step, with discharge power lower than 10 W, toluene removal of CuCeZr/A is slightly higher than that of CuCeZr/T, whereas, CO_2 selectivity exhibits a converse trend. NTP plays a dominant role and the catalyst is not activated completely. Much oxygen vacancy and lattice oxygen in CuCeZr/T, corresponding to enhancement of reactive oxygen mobility, can improve CO_2 selectivity to some extent. However, the improvement is limited due to the low background temperature caused by discharge. Generally, under low input discharge power, CO_2 selectivity for all the catalysts is significantly lower than the removal rate, which can be explained by the fact that the active species of NTP in this region attack the toluene molecules non-selectively which results in low CO_2 selectivity.

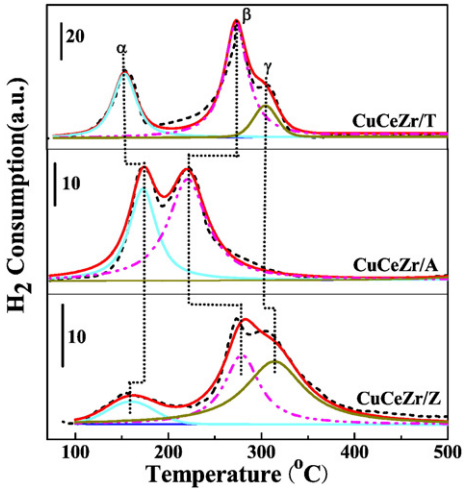

Fig. 2. H_2-TPR profiles of catalysts.

The second step, with the input discharge in the region of 10–25 W, catalysts can be activated by the gradually increase of background temperature, and toluene can be decomposed by the combination of plasma and catalyst. Fig. 3 shows that both toluene removal and CO_2 selectivity increase rapidly with increase of discharge power. The toluene removal for CuCeZr/T is higher than that for CuCeZr/A, while the values of CO_2 selectivity for both catalysts are very close.

The third step, with the input discharge power higher than 25 W, toluene removal rate increases slowly with the value for CuCeZr/T apparently higher than that for CuCeZr/A, and CO_2 selectivity for CuCeZr/T increases rapidly and surpasses CuCeZr/A. For instance, with discharge power increases from 25 to 42 W, toluene removal for CuCeZr/T increases from 98.2% to 100%, while the corresponding CO_2 selectivity increases from 64.8% to 94.2%. On the one hand, the background temperature further increases in the reactor through joule heating, dielectric loss, and gas heating in the plasma channel with the migration of electrons and ions [20], and it can activate the catalyst owing to the thermal chemistry. On the other hand, with the increase of input discharge power, plasma can activate catalyst gradually by changing the physicochemical properties of the catalyst, formation of hot spots, lowering the activation barrier and changing the reaction pathways, hence the catalyst's role becomes much more important or dominant. Moreover, species like ·O, ·N, etc., can interact directly with toluene resulting in an enhancement of toluene removal and CO_2 selectivity [21,22].

The energy yield of toluene removal was analyzed using removal quality of toluene divided by discharge power. The energy yield for

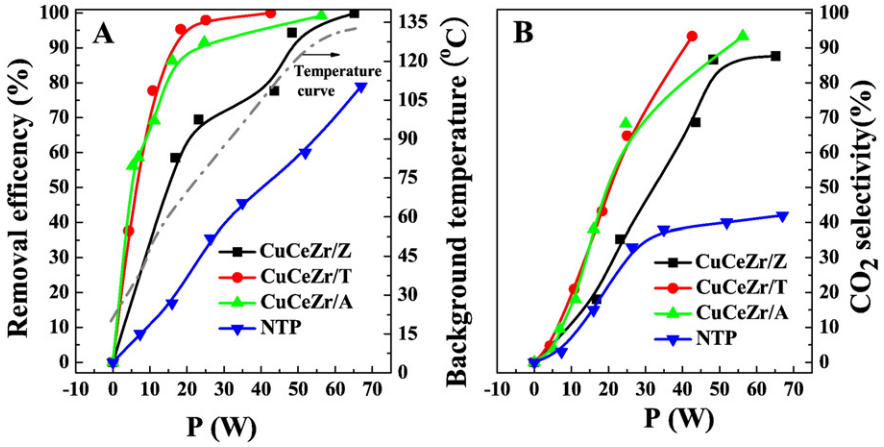

Fig. 3. Toluene removal, background temperature (A) and CO_2 selectivity (B) as a function of discharge power in the NTP-catalysts and pure NTP systems.

pure NTP is significantly lower than that for plasma-catalyst system, and the values stabilize at about 4 g/kWh (Fig. S4). The introduction of catalyst in plasma zone can distinctly improve the energy yield, which decreases with the increase of toluene removal ratio and CO_2 selectivity. Obviously, the energy yield for CuCeZr/Z exhibits lower value compared with CuCeZr/T and CuCeZr/A, probably owing to the relative small pore size restricting the development of micro-charge in inside the pores, less lattice oxygen and low reducibility. With removal rate exceeds 62% and CO_2 selectivity higher than 11%, the energy yield for CuCeZr/T is superior to that for CuCeZr/A in accordance with the results of toluene removal and CO_2 selectivity.

4. Conclusions

Toluene removal by using DBD combined with CuCeZr/Z, CuCeZr/T and CuCeZr/A catalysts was investigated. The presence of Cu-Ce-Zr based catalysts can significantly enhance the toluene removal and CO_2 selectivity. Toluene was decomposed synergistically by plasma and catalyst, and the process can be divided into three steps. At the initial DBD discharge, the process was dominated by plasma. Owing to the large pore size, more oxygen vacancy and lattice oxygen, the CuCeZr/T exhibited the excellent toluene removal, selectivity to CO_2 and energy yield, with the discharge enhancing in the second and third steps.

Acknowledgment

This work was supported by the National Natural Science Foundation of China (21307088) and the Young Innovation Fund of Tianjin University of Science & Technology (2015LG04).

Appendix A. Supplementary data

Supplementary data to this article can be found online at http://dx.doi.org/10.1016/j.catcom.2016.12.024.

References

[1] S. Zuo, F. Liu, R. Zhou, C. Qi, Catal. Commun. 17 (2012) 118–125.
[2] W. Tang, X. Wu, S. Li, W. Li, Y. Chen, Catal. Commun. 56 (2014) 134–138.
[3] A.M. Vandenbroucke, R. Morent, N.D. Geyter, C. Leys, J. Hazard. Mater. 195 (2011) 30–54.
[4] H.H. Kim, Y. Teramoto, N. Negishi, A. Ogata, Catal. Today 256 (2015) 13–22.
[5] R. Qu, X. Gao, K. Cen, J. Li, Appl. Catal. B Environ. 290 (2013) 142–143.
[6] X. Zhu, X. Gao, R. Qin, Y. Zeng, R. Qu, C. Zheng, X. Tu, Appl. Catal. B Environ. 293 (2015) 170–171.
[7] F. Bin, C.L. Song, G. Lv, J. Song, S.H. Wu, X.D. Li, Appl. Catal. B Environ. 532 (2014) 150–151.
[8] B.D. Rivas, R. Lo'pez-Fonseca, C. Sampedro, J.I. Gutierrez-Ortiz, Appl. Catal. B Environ. 90 (2009) 545–555.
[9] S. Li, Q. Hao, R. Zhao, D. Liu, H. Duan, B. Dou, Chem. Eng. J. 285 (2016) 536–543.
[10] F. Bin, X. Wei, B. Li, K.S. Hui, Appl. Catal. B Environ. 162 (2015) 282–288.
[11] Q. Deng, T. Ren, B. Agula, Y. Liu, Z. Yuan, J. Ind. Eng. Chem. 20 (2014) 3303–3312.
[12] J.F. Nastaj, B. Ambrozek, J. Rudnicka, Int. Commun. Heat Mass Transfer 33 (2006) 80–86.
[13] H.L. Chen, H.M. Lee, S.H. Chen, M.B. Chang, S.J. Yu, S.N. Li, Environ. Sci. Technol. 43 (2009) 2216–2227.
[14] J.L. Ayastuy, A. Gurbani, M.P. González-Marcos, M.A. Gutiér-rez-Ortiz, Int. J. Hydrog. Energy 37 (2012) 1993–2006.
[15] W. Tang, X. Wu, G. Liu, S. Li, D. Li, W. Li, Y.J. Chen, Rare Earths 33 (2015) 62–69.
[16] D. Romero, D. Chlala, Y. Labaki, M.S. Royer, Catalysts 5 (2015) 1479–1497.
[17] M. Labaki, J.F. Lamonier, S. Siffert, A. Aboukais, Thermochim. Acta 427 (2005) 193–200.
[18] K. Hensel, S. Katsura, A. Mizuno, IEEE Trans. Plasma Sci. 33 (2005) 574–575.
[19] K. Hensel, Eur. Phys. J. D 54 (2009) 141–148.
[20] F. Bin, X. Wei, T. Li, D. Liu, Q. Hao, B. Dou, Proc. Combust. Inst. (2017) http://dx.doi.org/10.1016/j.proci.2016.06.181.
[21] A.A. Assadi, A. Bouzaza, C. Vallet, D. Wolbert, Chem. Eng. J. 254 (2014) 124–132.
[22] A.A. Assadi, A. Bouzaza, D. Wolbert, J. Photochem. Photobiol. A 310 (2015) 148–154.